

Menon A, Waller N, Hu W, Hayhurst AN, Davidson JF, Scott SA.

[The combustion of solid paraffin wax and of liquid glycerol in a fluidised bed.](#)

Fuel 2017, 199, 447–455.

Copyright:

© 2017. This manuscript version is made available under the [CC-BY-NC-ND 4.0 license](#)

DOI link to article:

<https://doi.org/10.1016/j.fuel.2017.02.045>

Date deposited:

17/03/2017

Embargo release date:

14 March 2018



This work is licensed under a

[Creative Commons Attribution-NonCommercial-NoDerivatives 4.0 International licence](#)

The combustion of solid paraffin wax and of liquid glycerol in a fluidised bed

A. Menon^a, N. Waller^a, Wenting Hu^{b,c}, A.N. Hayhurst^{a*}, J.F. Davidson^a, S.A. Scott^b

a Department of Chemical Engineering and Biotechnology, University of Cambridge, Pembroke St, Cambridge CB2 3RA, England

b Department of Engineering, University of Cambridge, Trumpington St, Cambridge CB2 1PZ, England

c Now at: School of Chemical Engineering and Advanced Materials, Newcastle University, Newcastle NE1 7RU, UK

* Corresponding author, Tel.: + 44 1223 334790; fax: +44 1223 334796

E-mail address: anh1000@cam.ac.uk (A.N. Hayhurst)

HIGHLIGHTS

- In a hot bed of alumina sand, fluidised by air, paraffin wax burns like a plastic
- When wax is fed on top of a bed, at least half its carbon-content ends up as soot
- If wax is fed low down such a bed, no soot is produced – only CO or CO₂
- If glycerol enters low down a bed, it burns to CO or CO₂, without soot appearing
- Bubbles of fuel and air burn in a bed > 800°C, but explode above a cooler bed

ABSTRACT

Two fuels were burned in electrically heated beds of alumina sand, fluidised by air. The fuels were: (i) paraffin wax, which is a solid containing 100% volatile matter and (ii) glycerol, a liquid, whose potential as a fuel needs assessing. The bubbling fluidised beds were held in the range 400 - 900°C. Pieces of paraffin wax burned like a plastic, so when fed on top of a bed, the wax floated and generated clouds of soot. Soon, it then sank into the bed. When the sand was below ~ 800°C, combustion occurred noisily in exploding

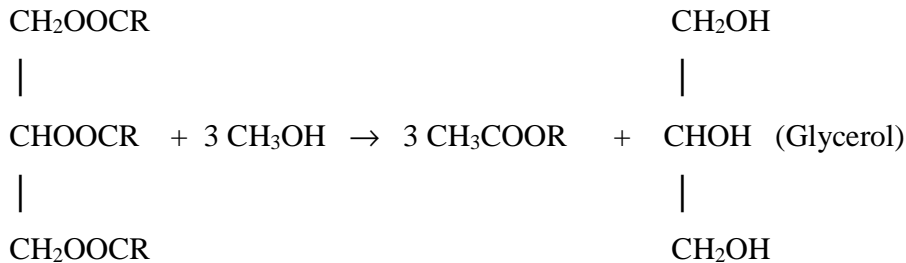
bubbles leaving the bed. In beds hotter than $\sim 800^{\circ}\text{C}$, combustion proceeded in bubbles fairly low in the bed and was controlled by the mixing of hydrocarbon vapours (from the wax) with the fluidising air. If wax were fed half way up a bed, bubbles of hydrocarbon vapours were quickly produced; they ascended and mixed with the fluidising air. In a bed below 800°C , combustion mainly occurred noisily in bubbles just after leaving the bed, but in a hotter bed, there was quieter burning in smaller bubbles, before they reached the top of the bed. Glycerol behaved similarly, when fed into the middle of a bed. Thus bubbles of glycerol vapour were formed; they mixed with air ascending the bed as either bubbles or percolating between particles. Again bubbles exploded noisily at the top of a bed below 800°C . With the bed above 800°C , glycerol burned inside smaller bubbles below the bed's upper surface. No soot was observed when burning glycerol in such a hot bed, yielding CO and CO_2 as the only products of combustion. It appears that burning glycerol cleanly in a hot fluidised bed is a feasible proposition.

1. Introduction

Fluidised beds, because of the rapidity of both heat and mass transfer inside them, make efficient and particularly compact combustors of solids, such as coal [1, 2], biomass [3, 4] and municipal waste [5 – 7]. By comparison they have not been used for burning liquid fuels. One exception is that Stubington and Davidson [8] burned kerosene in a fluidised bed of sand. They fed liquid kerosene through a cooled tube to the bottom of a hot bed fluidised by air and found a plume of hydrocarbon vapour rising upwards from where the fuel entered the sand. It was clear that combustion was controlled by the mixing of fluidising air with this column of vapour ascending from the fuel's point of entry. Quite strikingly, mixing was often slow enough for the plume of kerosene vapour to penetrate unburned into the freeboard above the bed. As for other studies of liquid fuels, only heavy fuel oils, some of them extremely heavy, have been burned in fluidised beds, usually of silica sand [9 – 17].

Glycerol is a potential liquid fuel, which is produced in quantities exceeding the demand for it. Glycerol arises as a by-product in the manufacture of biodiesel fuels by the transesterification of triacylglycerides (fats, vegetable oils or lipids) into methyl esters of

fatty acids. This process involves the triglyceride reacting with methanol (usually base-catalysed using NaOH or KOH) to yield biodiesel (CH_3COOR) and glycerol in:



It is noteworthy that for every tonne of biodiesel manufactured, 100 kg of glycerol are produced. Crude glycerol (usually called glycerine) contains methanol, water and soaps [18], because of a parallel, side-reaction between the triacylglycerine and the hydroxide catalyst. Normally glycerol poses problems as a fuel. It has a calorific value of only ~ 18 MJ/kg, compared to 43 and 44.4 MJ/kg for kerosene and gasoline, respectively. Even so, glycerine does have economic value as a fuel. Difficulties with burning it in a conventional manner include its high auto-ignition temperature ($\sim 370^\circ\text{C}$, compared with 220°C for octane) and its relatively high viscosity: at 20°C its dynamic viscosity is 1400 times that of water. This makes glycerol very difficult to atomise in a conventional burner. Another concern, when burning glycerine in an industrial burner, is the production of highly toxic acrolein and related pollutants [19].

This study is apparently the first one burning pure glycerol in a fluidised bed; the fluidised particles were alumina sand (density 3450 kg/m^3). Only batch additions of the liquid were investigated. Apart from visual observations, measurements were made of the temperature in the bed and the concentrations of O_2 , CO and CO_2 in the gas leaving the reactor. Comparisons were made with the combustion of paraffin wax, *i.e.* a solid containing 100% volatile matter, whose burning is likely to bear similarities to that of a liquid like glycerol.

2. Apparatus

The fluidised bed has been described [20], so only salient details are given here. The sand was contained in a stainless steel tube (length 1.13 m, i.d. 78 mm). At the bottom was a stainless steel distributor, perforated with 37 evenly spaced holes (i.d. 0.4 mm),

through which air flowed from the wind-box below. The alumina sand (sieved dry to 355 – 425 μm) rested on the distributor to a depth of 103 mm, when the sand was not fluidised. Air was fed to the bed from the laboratory's supply of compressed air; its flowrate was controlled by a needle-valve and measured with a calibrated rotameter. The steel tube housing the bed was surrounded by electric heating coils and then fire-bricks to provide thermal insulation.

A type K thermocouple, in the middle of the fluidised particles, was connected to a controller capable of maintaining the bed at a pre-set temperature up to $\sim 950^\circ\text{C}$. Typically the flowrate of air through the bed was ~ 0.2 litre/s, measured at room temperature and atmospheric pressure; this corresponds to a superficial velocity in the bed of $U = 0.169$ m/s at 900°C . The minimum value of U for incipient fluidisation at 900°C was estimated using the correlation of Wen and Yu [21] to be $U_{mf} = 0.066$ m/s, so $U/U_{mf} = 2.6$. This corresponds to a bubbling fluidised bed, as was seen to be the case from visual observations of the top of the bed. The value of U/U_{mf} was kept between 2.0 and 3.1 in the experiments described below.

The off-gases from the bed were sampled through a stainless steel tube (i.d. 4.57 mm; o.d. 6.35 mm). The sample passed continuously first through a drying tube containing fresh, anhydrous CaCl_2 to remove moisture and then through a train of instruments to measure the concentrations of O_2 (using a paramagnetic sensor) and of CO and CO_2 with infra-red analysers. In addition, it was possible to measure the concentration of CH_4 in the off-gases. Such sampling was driven by a pump; the flow rate entering the sampling train was ~ 0.5 litre/min, as measured at laboratory conditions. All concentrations were recorded by a data logger at a frequency of 5 Hz. The measuring instruments were calibrated using a gas of known composition containing O_2 or CO and CO_2 in N_2 .

Two fuels were burned. Weighed particles of paraffin wax (a heavy alkane of C_{20} – C_{25} , melting point $\sim 55^\circ\text{C}$, boiling point $\sim 390^\circ\text{C}$, density ~ 900 kg/m^3) were dropped from a glass dish onto the top of the glowing hot fluidised bed of alumina particles. Alternatively, a known mass of wax was inserted into a hollow, cylindrical, stainless steel capsule (tube's length 30 mm, i.d. 12.7 mm, o.d. 16 mm), sealed with two stainless steel end-caps. The capsule was attached to the end of a stainless steel chain and rapidly

dropped into the hot bed. The length of the chain controlled how far down the bed the capsule settled. Of course, the capsule was rapidly heated, so the wax boiled and blew off the end-caps, which were tied to the capsule with loose, stainless steel wire, so that the capsule and its end-caps were easily retrieved after an experiment. In this way a known mass of wax was added to a bed at a fixed temperature and at a particular height above the bed's distributor. The other fuel studied was vegetable glycerine, which is almost pure glycerol (melting point 17°C, boiling point 290°C, auto-ignition temperature 425°C, density 1,260 kg/m³ at 20°C). Samples of glycerol were put into the hot bed at a known height using the capsule and chain. Again, the capsule's end-caps were blown off, enabling the glycerol to escape into the hot bed. Adding the capsule, its contents and the chain, to a bed temporarily cooled the fluidised particles by ~ 20°C. Afterwards, the bed's temperature recovered in less than 1 min.

3. Results and Discussion

3.1 Combustion of paraffin wax dropped onto the top of a hot bed

Some continuously measured concentrations of O₂, CO and CO₂ in the off-gas from a bed at 900°C are shown in Fig. 1, for two consecutive batches (each 0.2 g) of paraffin wax simply dropped on top of the red-hot, fluidised sand. Any of the mole fractions of CO and CO₂ shown in Fig. 1, when multiplied by the total molar flow rate of gas passing through the bed, yields the rate of production (in mol/s) of the particular gas inside the bed. Also, the area under a peak of CO or CO₂, when multiplied by the total molar flow rate of the fluidising gas, gives the total number of moles of that gas produced by burning the known mass of paraffin wax. Such a measurement is not affected by the detectors for the gases having a finite response time. Areas under peaks were derived by numerical integration using the trapezium rule. For O₂, the number of moles, which have reacted, was derived from the "missing area" associated with the drop in its mole fraction seen in Fig. 1. That the minimum in [O₂] in Fig. 1 occurs slightly after the maxima in [CO] and [CO₂] shows that the O₂ detector is slightly slower than those for CO and CO₂. Also, it is clear from their rise-times, that the mole fractions of CO and CO₂ were being measured with response times less than ~ 4 s. Fig. 1 enables the burn-out time to be estimated for the wax added to the bed. In this case in Fig. 1, the burn-out time looks to be as long as ≈

45 s. Interestingly, the burn-out time did not vary significantly with the temperature of the bed over the range 400 to 900°C, when the burn-out time was consistently 42 ± 5 s for 0.1 g of wax dropped on top of a bed. Fig. 1 shows that, except for the final stages of burning, the rate of production of CO in this case exceeds that for CO₂. However, this is not always the case; in fact, it will be seen below that there are situations, where more CO₂ appears than CO. Both the rates of production of CO and CO₂ rise to maxima and then fall steadily. Likewise, the rate of consumption of O₂ grows to a maximum value and subsequently falls to zero. Of course, these measurements in Fig. 1 refer to a mixture of the gas, which left the bed as bubbles (*i.e.* the bubble phase), and that which ended up percolating between the particles of alumina (*i.e.* the particulate phase).

FIGURE 1 HEREBABOUTS

The visual observations are described first. Upon dropping a pellet of paraffin wax onto the top of a hot bed, clouds of soot left the bed. Next, a yellow (*i.e.* sooting) flame was sometimes seen emerging from the bed. These flames were tallest for the hottest bed at 900°C and were shorter in length, when less wax was added. Some flames were as long as 1 m. In addition, bubbles of gas were sometimes seen (from above the bed) to produce a flame on leaving the bed and also make a fairly loud “popping” noise, which was really a sequence of several ‘pops’. Such noisy flames were present, when the bed was at 400 - 600°C. When a sooty diffusion flame was seen initially, the “popping noises” followed afterwards. Fewer, quieter, “popping” sounds were heard at 800°C and hardly any at 900°C.

3.2 Ignition of bubbles

These loud noises have been reported before [22–27]. The nature of these explosions is not clear, but there is evidence that sand particles inhibit combustion by providing surfaces, on which free radicals recombine [22–27]. Thus, inside a bed, combustion usually occurs only in bubbles, which grow in diameter by coalescing with one another [28], whilst ascending the bed. Bubbles rise with a velocity $U_b = 0.71\sqrt{(gD_e)}$ m/s, where g is the acceleration due to gravity and D_e is the bubble’s equivalent diameter [29]. The bubbles leaving a bed were seen to have a diameter, $D_e \approx 10$ mm, so their rise velocity

was then ≈ 0.22 m/s at the top of the bed. This should be compared with the interstitial velocity of the gas percolating between the particles; this is $U_i = U_{mf} / \varepsilon$, where ε is the voidage fraction in the particulate phase. The value of ε is close to 0.4 [29], so the interstitial velocity $U_i = 0.066/0.4 = 0.165$ m/s, at 900°C: this makes U_i slightly less than U_b . In that case, inside such a bubble, just before it leaves a bed, there is a small, horizontal toroidal ring [29], within which gas merely circulates in a vertical direction, without escaping. The gas inside the toroid is well-stirred. Through the rest of the bubble, gas rushes vertically into the particulate phase ahead [29] of the bubble. The fraction of a bubble occupied by the toroidal, recirculating region, is larger in a bigger bubble [29] and *vice versa*.

In general, a gaseous mixture of fuel and oxidant, when **stagnant**, ignites only after a certain induction time, called the ignition delay, characteristic of chain reactions leading to an explosion [30, 31]. The ignition delay is very sensitive to the temperature [30, 31], being smaller at higher temperatures and pressures; it varies as $A \exp(B/T)$, where A is a function of the concentrations of the gaseous fuel and oxidant, B is a constant and T is absolute temperature. For example, a mixture of a C_7 hydrocarbon in air at 800°C has an ignition delay of $\approx 1 - 5$ ms [30]. In a fluidised bed, the ignition of a bubble is different, in that the ignition delay is usually prolonged by the flow of gas straight through the bubble, *i.e.* the through-flow [29]. This is because the through-flow removes enthalpy and intermediate species (free radicals), which otherwise would sustain the chain reactions of combustion [30, 31]. The question arises as to when does a bubble of an explosive mixture ignite in a fluidised bed? The answer depends on the temperature: (i) First, consider a hot bed above 850°C, so the ignition delay is brief. Then small bubbles will ignite low down such a hot bed, if the residence time of gas moving upwards through a bubble and along its vertical axis is longer than the relevant ignition delay [32]. In this case, only bubbles larger than a certain size can ignite in such a hot bed. Moreover, the critical size for an exploding bubble will be smaller at higher temperatures. (ii) Next, with a bed at 700 – 850°C, a bubble containing hydrocarbons and air can ignite, while rising up the bed, provided the bubble has become large enough for the toroid (of confined gas inside it) to become a significant fraction of a bubble. This occurs when the bubble has

become so big that U_b is comparable to U_i . In this case, there is a second requirement that the bubble exists undisturbed, before its next collision with another bubble, for longer than the relevant ignition delay. Thus, again ignition occurs when the bubble reaches a critical size, which is larger at smaller temperatures. (iii) At the lowest temperatures in this study (400-700°C), the ignition delay is so long that bubbles do not become large enough to ignite inside one of these shallow beds. In that case, bubbles only ignite on leaving the bed and do so noisily, because the bubbles have become bigger than ≈ 10 mm. That these bubbles lose their through-flow and also decelerate on disengaging from the bed actually helps their ignition and probably accounts for the noisy combustion observed above beds below 800°C. These general considerations, of when a bubble of hydrocarbon vapours and air ignites, are considered further below.

It is also worth noting that U (the velocity of the gas above the bed) is ~ 0.169 m/s at 900°C. However, at 800°C the value of U is only a little smaller than this value for 900°C, and is also less than the burning velocity [30, 31] of a mixture of air and hydrocarbons [33] at 800°C. The consequence of this is that a flame usually moves downwards through the freeboard and “sits” stably on top of the fluidised particles, instead of being blown out of the tube housing the bed. Of course, inside a fluidised bed, gas velocities are higher than above the bed, because of the presence of solid particles; the result is that a flame in the particulate phase is blown out of the bed and ends up sitting on top of the sand.

3.3 Burning of paraffin wax continued

That a sooty diffusion flame was usually seen straight after adding paraffin wax indicates that hydrocarbon vapours are at first produced so rapidly that they do not mix much with the fluidising air. Instead, the cloud of hot hydrocarbons forms soot very rapidly [33] in an atmosphere almost devoid of oxygen. However, the subsequent “popping” sounds indicated that the hydrocarbon vapours were mixing, at least to a slight extent, with the fluidising air. As to what happens to the paraffin wax, these “popping” noises do suggest that, after an interval, “blobs” of molten paraffin wax had descended lower in the fluidised bed. This would result in hydrocarbon vapours from the evaporating wax having more time to mix in the bed with the fluidising air. Bubbles of air mixed with vapour from the wax then ignited explosively on leaving the top of the bed.

This is reminiscent of the burning of polymer pellets, when dropped on a hot fluidised bed of sand [34]. In that case, the polymer pellets melted and also acquired sand on top of them [35], causing them to sink. The noises suggested that bubbles of a mixture of hydrocarbon vapours and air were not igniting inside the bed, but did so, explosively, when the bubbles disengaged from the bed. This is in line with the bubbles rising up a bed below $\approx 800^{\circ}\text{C}$ being too small to ignite [22].

FIGURE 2 HEREABOUTS

Fig. 2 shows burn-out times for single and multiple particles of different masses of paraffin wax dropped on top of beds at $400 - 900^{\circ}\text{C}$. For this, small pieces of wax were heated beforehand to form a melt. As the melt later cooled, it was rolled and shaped to form one larger, round particle. Fig. 2 shows a surprising trend of the burn-out time increasing with the bed's temperature. This possibly unexpected result could derive from the fact that to maintain U/U_{mf} constant at close to 2.6, U was smaller at higher temperatures, because U_{mf} is smaller for a hotter bed. The result is that mass transfer from an evaporating 'blob' of wax (molten on its exterior) is reduced by lowering both U_{mf} and U . The burn-out times in Fig. 2 appear to be usually the same for one pellet and for several of the same total mass. This is possibly not true at the highest temperature of 900°C , where single, large particles, quite counter-intuitively, can burn quicker than several smaller ones. Here it is worth noting that the burn-out time of a pellet of a polymer in a fluidised bed is the same [34] for polymer fed as one pellet and as many smaller ones of the same total mass. Interestingly, polymer pellets were actually observed [34] to sink into a fluidised bed of hot quartz sand immediately after landing. Finally, it is clear from Fig. 2 that the burn-out time increases with the mass of wax being burned. However, the increase is not as much as expected from models for a shrinking core or for a burning, spherical liquid droplet [36]; these models predict that the burn-out time depends on the square of the particle's initial diameter, *i.e.* its mass raised to the power $2/3$.

FIGURE 3 HEREABOUTS

Fig. 3 is a plot of the fraction of the carbon in the paraffin wax (assumed to contain only carbon and hydrogen in the atomic ratio CH_2), which was detected as a gaseous

oxide, *i.e.* either CO or CO₂, in the off-gases from beds at different temperatures. Also in Fig. 3, the mass of wax added was varied. Several points emerge from Fig. 3. First, much less than half the carbon in the paraffin wax was oxidised to either CO or CO₂. At most, 35% of the carbon was oxidised at 900°C. This is in line with observations of clouds of soot leaving the fluidised bed. For soot to form in this situation, the wax must melt and boil rapidly, producing a stream of hydrocarbon vapours, which heat up without mixing much or being oxidized by the fluidising air. Secondly, Fig. 3 shows that the fractional conversion of the wax's carbon to CO and CO₂ increased with the temperature of the bed. Finally, the fraction of the wax undergoing oxidation increased, when more wax was added. This is probably connected to the burn-out time also increasing, when more wax was burned, as seen in Fig. 2.

These observations so far are, in line with a pellet of wax melting very quickly (melting point $\sim 55^\circ\text{C}$) on first being dropped on top of a hot fluidised bed. There the wax particle will continue to heat up. It is important to evaluate the ratio of (i) the internal resistance to heat transfer inside a solid sphere to (ii) the external resistance to heat transfer from the bed to the hot sphere; this ratio is the Biot number, $\text{Bi} = hd/6\kappa$ [37]. Assuming the external heat transfer coefficient $h = 500 \text{ W m}^{-2} \text{ K}^{-1}$ [38] for a sphere of diameter $d = 7.5 \text{ mm}$ (weighing $\sim 0.2 \text{ g}$ for a sphere of paraffin wax), and the thermal conductivity, κ , of the solid wax is $0.28 \text{ W m}^{-1} \text{ K}^{-1}$ [39], yields $\text{Bi} \sim 2.2$. This is just large enough for internal heat conduction and temperature gradients inside the waxen sphere to control its rate of heating. Thus there would be little difference in temperature between the wax's exterior and the bed [37]. Such a conclusion is firmer for particles larger than 7.5 mm. However, vaporisation inevitably begins quickly, so that a wax particle becomes surrounded by a gaseous envelope of hydrocarbon vapour, ensuring that there are temperature gradients around the evaporating particle, as well as within it. The process of evaporation takes several seconds, just as a similarly sized sphere of solid CO₂ takes $\sim 8 \text{ s}$ to evaporate in a fluidised bed at room temperature [40].

This picture of a near-spherical particle of wax at first floating on top of a hot fluidised bed and generating soot is soon modified by the fact that fluidised particles are continuously ejected a little distance into the freeboard and then land on top of the wax.

This means that, very quickly, alumina particles accumulate on top of the sticky blob of wax and a cushion of fluidising air forms beneath the wax [35]. Evaporation ensures that around a wax particle there is a cloud of hydrocarbon vapour, which reduces both heat and mass transfer and consequently the rate of evaporation. Also, alumina particles become embedded in the wax particle, so it sinks into the fluidised bed. The hydrocarbon vapours now have more chance of mixing with the fluidising air and consequently of burning to produce CO and CO₂, rather than soot. Larger wax particles sink for longer times before completely evaporating, implying that bigger particles descend deeper; thus more of their carbon-content ends up as CO or CO₂, because within the bed there is better mixing of hydrocarbon vapours with the fluidising air. At this stage, as to why the burn-out times in Fig. 2 are similar for large and smaller particles of the same total mass could be a consequence of small sticky blobs of melting wax coalescing soon after landing on top of a hot bed. As for why Fig. 3 implies that less soot is produced in a hotter bed, perhaps a particle of wax floats for a shorter time in a hotter bed and then sinks deeper down such a hot bed.

FIGURE 4 HEREABOUTS

Fig. 1 showed that the ratio $[CO]/[CO_2]$ was highest immediately after adding wax to a bed, but subsequently fell. The ratio is a crude indicator of how fuel-rich is a particular mixture of combustible gases. Fig. 4 shows plots of average values of this molar ratio for different amounts of wax added to beds at 400 to 900°C. Clearly, there is a trend to have more CO in the off-gases than CO₂, when more wax was added to the bed, but its variation with temperature is complex. Fig. 2 shows that increasing the temperature gave longer burn-out times, because wax sinks deepest into the hottest bed. This implies that $[CO]/[CO_2]$ might decrease at higher temperatures, because then more air contacts the hydrocarbon vapours. However, increasing the temperature, as mentioned above, meant lowering U slightly to maintain U/U_{mf} constant. This decrease in the flow of air would tend to favour the production of CO over CO₂. As for other contributing factors, the effect of temperature on transport properties is not likely to be a major factor for Fig. 4, but radiative heating of a burning particle will be most important at 900°C. If heat transfer alone controlled the rate of evaporation, the rate of production of fuel vapour and

also the ratio, $[\text{gasified fuel}]/[\text{O}_2]$, in the bed would increase with temperature, leading to higher $[\text{CO}]/[\text{CO}_2]$. If, however, evaporation were mass-transfer controlled, raising the temperature of the bed would mean that both U and U_{mf} , and consequently also the convection of hydrocarbon vapours into the bed, were reduced. Such a lowered rate of evaporation would probably lead to a smaller $[\text{CO}]/[\text{CO}_2]$. All this means that the rise of $[\text{CO}]/[\text{CO}_2]$ in Fig. 4 with temperature looks to be a consequence of enhanced heat transfer, as well as U and U_{mf} being reduced. The final drops at 900°C in Fig. 4 have to be explained by the burn-out time increasing with the bed's temperature.

In summary, it looks as if a piece of paraffin wax does float briefly after being dropped on top of a hot fluidised bed. The subsequent rate of evaporation is high enough to produce clouds of soot. However, the sticky wax, molten on its exterior, soon sinks, because it is weighed down by ejected sand falling on top of it. The result is that boiling of the sunken particle of wax produces hydrocarbon vapour, which appears as bubbles inside the bed. These bubbles rise up the bed and mix with air either percolating through the alumina particles or ascending as bubbles. There is also the fact that combustion of mixtures of hydrocarbons and air is suppressed in the particulate phase. Normally such burning does not occur below $\sim 800^\circ\text{C}$ [22], but it can occur explosively, when the largest bubbles of the mixture leave the top of the bed [24], thereby emitting a loud and repeated “popping” noise. There are thus many stages for the combustion of the hydrocarbon vapours; perhaps the slowest process is the mixing (with air) of hydrocarbons in a plume of bubbles rising from a sinking particle of wax. Finally, it appears from Fig. 2 that the burn-out time is independent of whether wax is added as one particle or several smaller ones. It is likely that, soon after falling on to a hot bed, the small sticky particles collide and coalesce, before the resulting wax pellets have sand embedded in them. Then these big pieces of wax descend as a single entity into the bed.

3.4 *Combustion of paraffin wax inserted into the middle of the bed*

Paraffin wax was added to the middle of the bed at 80 mm above the distributor using the capsule and chain, described in Section 2. Thus a weighed amount of wax was injected into the bed at a selected height above the distributor. The bed was at 500, 650, 800 or 900°C; U/U_{mf} was held constant at 2.4. No soot was observed, when wax was

added this way. However, “popping” noises were again heard, but small blue flames (*i.e.* non-sooting) were also seen above the beds at 500 and 650°C. There were fewer “popping” sounds from beds at 800 or 900°C. In these experiments, the wax must heat up rapidly, melt and then evaporate. The rise in pressure within the capsule would soon blow off the capsule’s end-caps. Evaporation of the molten wax might be aided by its liquid pouring from the capsule into the bed.

FIGURE 5 HEREABOUTS

Fig. 5 shows the mole fractions, [CO] and [CO₂], after adding two successive batches of 0.1 g of paraffin wax to the middle of a bed at 800°C with $U/U_{mf} = 2.4$. The traces are similar in shape to those in Fig. 1, for paraffin wax added to the top of the bed; again the burn-out time is ≈ 45 s. This similarity of burn-out times suggests that the wax might have entered the bed from the capsule, almost entirely as a solid. It was, however, observed that no soot was produced. Popping noises, similar to those heard for the combustion of wax dropped on top of a bed, were heard for a period of time. Also, small, blue (*i.e.* non-sooting) flames were seen leaving the bed, when at 500 - 650°C. The absence of soot indicates good mixing of the fuel’s vapour with the fluidising air. It is worth noting that the ratio, [CO]/[CO₂], changes dramatically with time: thus, towards the end of burn-out, [CO] drops to become much smaller than [CO₂]. This effect is much more pronounced than in Fig.1.

FIGURE 6 HEREABOUTS

Fig. 6 gives plots of the burn-out times, measured when 0.10 g of paraffin wax was injected into the middle of the bed at different temperatures, with $U/U_{mf} = 2.4$. There is a modest increase of burn-out time with the temperature of the bed. This is probably on account of the flow-rate of gas through the bed, *i.e.* both U and U_{mf} , decreasing at higher temperatures. Such a trend, as discussed above, reduces the rates of both heat and mass transfer. Interestingly, these burn-out times in Fig. 6 exceed those in Fig. 2 for the same amount of paraffin wax (0.1 g) dropped onto the top of a hot bed, except at the highest temperature of 900°C, when they are similar. For Fig. 6 the wax was initially inside the capsule, so there would have been heat transfer from the capsule to the wax, followed by

mass transfer of vaporised wax from the capsule to the bed. Both these transfer processes prolong burning, but their effects are clearly less conspicuous at 900°C.

FIGURE 7 HEREABOUTS

Fig. 7 shows the results of measuring the areas under the plots of $[O_2]$, $[CO]$ and $[CO_2]$ like those in Fig. 5, for the same mass of wax added from the capsule. The outcome is shown in Fig. 7 as the fraction of the carbon, which subsequently was detected as CO and CO_2 . For these experiments, some problems were encountered from the zero of the detectors for CO and CO_2 drifting. This was coped with partly by using the measurements for $[O_2]$, together with measurements of the ratio $[CO]/[CO_2]$. The striking feature of Fig. 7 is that all the carbon was converted to CO and CO_2 , when paraffin wax was added from the capsule to the middle of the bed. This is in contrast to Fig. 3, where soot was produced and the yield of the oxides of carbon depended on the mass of wax burned and the temperature. Fig. 7 is in line with the accompanying observations of a blue flame and no soot being detected. As already noted, the burn-out times in Fig. 6 were consistently fairly long; this is likely to facilitate mixing of air and the hydrocarbon vapours from the evaporating wax. That many “popping” sounds were heard from beds at 500 or 650°C, but with fewer at 800 or 900°C, agrees with the observations of wax burning on top of a bed. Thus it appears that bubbles containing both air and hydrocarbon vapour might burn low inside a bed at 900°C, or even at 800°C, but only above the bed at lower temperatures. The lack of soot after injecting wax into the middle of the bed indicates that when wax was dropped onto the bed, soot was primarily formed whilst the wax floated and burned on top of the hot sand.

FIGURE 8 HEREABOUTS

Fig. 8 shows the ratio of the overall molar yields of CO and CO_2 , measured in the off-gases for the conditions of Fig. 7. Clearly the values are much lower than in Fig. 4, for wax added to the top of the bed, when some values of the ratio exceeded unity. In Fig. 8, values fall monotonically to zero at 900°C. That these values in Fig. 8 are smaller than in Fig. 4 indicates that mixing of fuel vapour and fluidising air was much improved by injecting the wax within the bed. That $[CO]/[CO_2]$ now falls with increasing temperature

in Fig. 8 could be a consequence of molten wax particles leaving the capsule and then falling deeper down a hotter bed, giving more time for hydrocarbon vapours to mix with fluidizing air. In this context, Figs 2 and 6 show the burn-out time being longer in a hotter bed.

3.5 Combustion of glycerol inserted batchwise into the middle of a hot bed

Different masses of glycerol were added from the capsule into the middle of the bed, at 80 mm above the distributor, at 500, 650, 800 and 900°C. For these investigations, liquid glycerol was pipetted into the capsule. The value of U/U_{mf} was kept constant at 2.4. The “popping” noises were again heard in beds at 500 and 650°C, but there were fewer such noises at 800 and 900°C. No flames were seen for less glycerol added, but a wide, steady, blue (*i.e.* non-sooting) flame was observed rising ≈ 50 mm above the bed for the highest quantity (0.50 g) added. This indicates that with 0.5 g added, glycerol vapours were burning as a flame either sitting on top of the bed or extending above it. The same could have been true for the vapours from paraffin wax sometimes burning either on top of or just above the bed. When the capsule was withdrawn, both end caps were seen to have blown off. The volume of vapour formed when burning 0.3 g of glycerol in a bed at 500°C and atmospheric pressure is estimated to be 0.21 litres. The internal diameter of the capsule was 12.7 mm, so bubbles of diameter ≈ 10 mm might be expected to form, giving some 420 bubbles at 500°C. Air percolating through the fluidised particles would mix with these hydrocarbon bubbles [30], leading eventually to combustion.

FIGURE 9 HEREABOUTS

Fig. 9, for glycerol, is analogous to Figs 1 and 5 for paraffin wax, in that it shows plots of the mole fractions, [CO], [CO₂] and [O₂], versus time when two batches of 0.3 g of glycerol were added consecutively from the capsule to the middle of the fluidised bed at 800°C with $U/U_{mf} = 2.4$. Fig. 9 shows that the burn-out time is ≈ 50 s for this amount of glycerol added to the middle of the bed. This is fairly similar to the burn-out time of ≈ 45 s noted in Fig. 5 for paraffin wax, also added to the middle of the bed at 800°C. This similarity might be a reflection of almost identical rates: (i) of heat transfer to the liquefied wax and liquid glycerol, inside the capsule, (ii) at which the fuel leaves the

capsule and (iii) of mixing of the ascending bubbles of the fuel-vapour with the fluidising air.

FIGURE 10 HEREABOUTS

Burn-out times for glycerol added to the middle of the bed are collected in Fig. 10 for different temperatures and quantities of glycerol added, but only for $U/U_{mf} = 2.4$. The times range from ~ 40 s to ~ 60 s. Burn-out times are slightly longer in a hotter bed; this is not a major effect, just like the gradual rise in Fig. 6 for paraffin wax added to the middle of the bed. More definite is the burn-out time lengthening with the mass of glycerol added. This might suggest that it takes time for the glycerol to leave the capsule, either as vapour or as liquid pouring into the bed. Maybe the liquid first boils and vapour leaves the capsule, whilst simultaneously being replaced with air. The glycerol vapour will, to some extent, be pyrolysed and enter the bed as many bubbles, as noted above. These bubbles of a complex mixture of hydrocarbons will then rise up the bed and mix with the fluidising air. The time for a bubble to rise to the top of a bed is no more than 1 s.

FIGURE 11 HEREABOUTS

Fig. 11 shows the fraction of the carbon (added as glycerol to the middle or bottom of the bed), which is detected as CO or CO₂ in the gas leaving the bed. That some values in Fig. 11 indicate a conversion slightly greater than 100% can be attributed to drift in the zero for the detectors, as noted in Fig. 7. The conclusion from Fig. 11 is simple and striking: all the carbon was oxidised to CO or CO₂, even when added to the middle of the bed. This means that mixing of the hydrocarbon vapours with fluidising air was good, although it must be recognised that glycerol contains equimolar amounts of carbon and oxygen. Thus there is enough oxygen in a molecule of glycerol to burn the carbon to CO, without soot being formed.

FIGURE 12 HEREABOUTS

Fig. 12 shows the molar ratio [CO]/[CO₂] in the off-gas, when different quantities of glycerol were burned in beds at various temperatures. There is little difference between the results for 800°C and 900°C. In these two hotter beds, the ratio [CO]/[CO₂] rises from zero to ~ 0.2 for 0.5 g of fuel added to the middle of the bed, when there is five times

more CO₂ produced than CO. Thus, combustion to CO₂ is almost complete, given that Fig. 11 showed that CO and CO₂ were the only products containing carbon. It is understandable that adding more glycerol to a hot bed, fluidised by air, resulted in combustion becoming more fuel-rich, thereby increasing the ratio [CO]/[CO₂]. The curve in Fig. 12 for 500°C is totally different from the others; adding more glycerol leads to relatively less CO, with the ratio falling from unity to the same value as for the other temperatures. This indicates that combustion is quite different with small amounts of glycerol added at 500°C. One would expect combustion at 500°C to occur noisily in bubbles after leaving the bed. It might be that at 500°C adding more glycerol results in better mixing of glycerol with the fluidising air. This might have happened if adding the least amount of glycerol at 500°C caused it all to evaporate and blow off the capsule's end-caps before the capsule had sunk far down the bed. In that case, adding more glycerol might enable the capsule to sink deeper in the bed. Alternatively, it could be that after ignition, the oxidation of CO to CO₂ is really slow at 500°C. It is known [31] that the burning of CO in O₂ is accelerated by the presence of hydrogenous species, which here originate in the fuel, glycerol. This leads to the rate of oxidation of CO to CO₂ being non-linear in the initial concentration of glycerol.

FIGURE 13 HEREABOUTS

Fig. 13 deals with these factors in a different way. Again, it displays plots of [CO]/[CO₂], this time when 0.3 g of glycerol was added from the capsule, either in the middle of the fluidised bed (80 mm above the distributor) or at the distributor. Fig. 13 shows that more CO was detected, when the glycerol was released in the middle of the bed, giving less time for the fuel and fluidising air to mix, whilst they rose up the bed. The observations in Figs 12 and 13 are consistent with bubbles igniting on leaving the bed at 500°C. In this situation, the complex kinetics [31] of the oxidation of CO might well be important. Otherwise, there is not a big difference between the observations at 650, 800 and 900°C. This confirms the previously noticed weak influence of temperature on the mixing of fuel and air. Fig. 13 might be compared with Fig. 8 for paraffin wax added to the middle of the bed. Figure 8 shows the ratio [CO]/[CO₂] decreasing in hotter beds; also, the ratio looks to be slightly higher for glycerol than for paraffin wax.

As a final experiment, glycerol was dropped onto the top of a hot bed of alumina sand fluidised by air. This produced considerably less soot than when paraffin wax containing a comparable amount of carbon was dropped onto the same bed. This must at least partly derive from a molecule of glycerol having a C/O ratio (on an atomic basis) of unity, so there is enough oxygen in glycerol to oxidise all its carbon to carbon monoxide. The rough criterion that C/O must exceed unity [33] for a particular mixture to produce soot seems to be satisfactory here.

4. Conclusions

Of the combustion situations explored above, the most complex was that involving one or more pieces of paraffin wax thrown onto the top of a hot, electrically heated bed fluidised by air. The hydrocarbon vapours from the wax were, of course, very fuel-rich and so initially produced a lot of soot, whilst the wax bounced around, floating on top of the fluidised particles of alumina. Fig. 3 shows the fraction of the carbon in the wax ending up as soot could be as high as 90 %, but that fell to ~ 65 % for a large piece added to a hot bed at 900°C. In this latter case, the large piece of wax acquired embedded inert particles and then fell deep into the bed. In that case, seen in Fig. 2, the burn-out time was longest and lasted for ~ 1 min. Another striking feature was that the burn-out time for several small particles of wax added simultaneously was the same as for one large piece of the same total mass. This was attributed to wax particles coalescing very soon after landing on top of a bed, *i.e.* when they were “sticky” and not yet covered with particles of alumina. Unexpectedly, the burn-out time for a piece of wax was longer in a hotter bed, but of the same U/U_{mf} . This was attributed to U_{mf} , and therefore also U , falling with temperature and consequently reducing heat and mass transfer between a wax particle and the hot bed. In addition, larger pieces of wax had more time to sink deeper into the bed, so the hydrocarbon vapours emitted had a better chance of mixing with the fluidising air and also of burning to CO or CO₂.

It is clear that bubbles of a mixture of hydrocarbon vapour and air have to reach a critical size, which depends on the temperature, in order to ignite. In a bed below 800°C, these sizes were not attained, so mixtures then burned noisily in bubbles when leaving the top of a bed. There, at the very top of a bed, the bubbles were largest and the particulate phase had a greater voidage than in the bulk of the bed, so the velocity of the gas

percolating between the particles was decreasing, as also was the velocity of the gas rising inside bubbles. This deceleration thus aids combustion, but the large volume of these exploding bubbles is an important factor generating the noise associated with their ignition. That these bubbles can explode well above a bed might indicate that bubbles decelerate gradually on leaving the bed, but actually retain their composition until igniting in the freeboard. In beds hotter than 800°C, combustion can occur relatively quietly inside smaller bubbles lower within a bed.

The combustion of paraffin wax, added to the middle of the fluidised bed, produced no soot, because bubbles of hydrocarbon vapours had time to mix with the fluidising air. Combustion in a bed below 800°C was again inhibited by either the bubbles being too small or the ignition delay too long, so burning was noisy and in bubbles disengaging from the top of the bed. In hotter beds, combustion proceeded more quietly below the top of the bed. This study has cast light on possible mechanisms for the ignition of inflammable bubbles in a fluidised bed.

Glycerol added to the middle of the bed burned in a very similar way to paraffin wax added to the same position. In this case, the glycerol evaporated and its vapour entered the bubble phase. There was mixing with air from the particulate phase, so that bubbles of glycerol and air either ignited at the very top of the bed, if the temperature was below 800°C or deeper down the bed in smaller bubbles, if the bed was hotter than 800°C. The production of soot did not seem to be a problem in this case, possibly because glycerol contains equimolar quantities of carbon and oxygen. It is accordingly clear that glycerol can be burned usefully in a fluidised bed, without soot being produced, provided the bed is hotter than 800°C. The continuous feeding of glycerol to one of these beds is currently under investigation, together with the characteristics of such combustion.

References

- [1] La Nauze R D, Combustion in Fluidised Beds, In: Advanced Combustion Methods, editor Weinberg F J, Academic Press, London, 1986, pp. 17 – 111.
- [2] Hoy H R, Gill D W, The combustion of coal in fluidized beds, In: Principles of Combustion engineering for boilers, editor Lawn C J, Academic Press, London, 1987, pp. 521 – 619.

- [3] Gomez-Barea A, Leckner B, Modeling of biomass gasification in fluidized bed, Prog. Energy Combust. Sci. 2010; 36; 444 – 509.
- [4] Werther J, Saenger M, Hartge E-U, Ogada T, Siagi Z, Combustion of agricultural residues, Prog. Energy Combust. Sci. 2000; 26; 1 – 28.
- [5] Cooke R B, Goodson M J, Hayhurst A N, The combustion of solid wastes as studied in a fluidized bed, Trans I Chem E (B) 2003; 8; 156 – 165.
- [6] Ogada T, Werther J, Sewage sludge combustion, Prog. Energy Combust. Sci. 1999; 25; 55 – 116.
- [7] Saxena S C, Jotshi C K, Fluidized-bed incineration of waste materials, Prog. Energy Combust. Sci. 1994; 20; 281 – 324.
- [8] Stubington J F, Davidson J F, Gas-phase combustion in fluidized beds, AIChE J 1981; 27; 59 – 65.
- [9] Okasha F M, El-Emam S H, Mostafa H K, The fluidised bed combustion of a heavy liquid fuel, Exp. Thermal and Fluid Sci, 2003; 27; 473 – 480.
- [10] Okasha F, Modeling of liquid fuel combustion in a fluidized bed, Fuel 2007; 86; 2241 – 2253.
- [11] Beacham B, Marshall A R, Experiences and results of fluidized combustion plant at Renfrew, J. Inst. Energy 1971; June; 59 – 64.
- [12] Faravelli T, Frassoldati A, Ranzi E, Miccio F, Miccio M, Modeling homogeneous combustion in bubbling beds burning liquid fuels, J. Energy Resources Technol. 2007; 129; 33 – 41.
- [13] Anthony E J, Lu D Y, The fluidised bed combustion of heavy liquid fuels, 16th Int. Conf. on FBC, 2001, Paper No. FBC 99 – 0141.
- [14] Borodulya V A, Dikalenko V I, Dobkin S M, Markevich I I, Fluidized-bed burning of volatiles and liquid fuel vapour, Heat Transfer Res., 1992; 24; 832 – 839.
- [15] Pillai K K, Elliott D E, The feasibility of heavy oil combustion in shallow fluid beds, J. Inst. Fuel 1976; Dec; 206 – 210.

- [16] Legros R, Lim C J, Brereton C M H, Grace J R, Circulating fluidized bed combustion of pitches derived from heavy oil upgrading, *Fuel* 1991; 70; 1465 – 1471.
- [17] Scala F, Miccio F, Miccio M A, 1-D zone model for the axial burning profile of liquid fuels in bubbling fluidized beds, *Fluidization XI* (Editors: Arena U, Chirone R, Miccio M, Salatino P) Engineering Conferences International, Brooklyn, 2004; pp. 835 – 842.
- [18] Yang F, Hanna M, Sun R, Value-added uses for crude glycerol, a byproduct of biodiesel production, *Biotechnology for Biofuels* 2012; 5; 1 – 10.
- [19] Bohon M D, Metzger B A, Linak W P, King C J, Roberts W L, Glycerol combustion and emissions, *Proc. Combust. Inst.* 2011; 33, 2717 – 2724.
- [20] Collier A P, Hayhurst A N, Richardson J L, Scott S A, The heat transfer coefficient between a particle and a bed (packed or fluidised) of much larger particles, *Chem. Eng. Science* 2004; 59; 4613 – 4620.
- [21] Wen C Y, Yu Y H, A generalized method for predicting the minimum fluidization velocity, *AIChE J* 1966; 12; 610 – 612.
- [22] Dennis J S, Hayhurst A N, Mackley I G, The ignition and combustion of propane/air mixtures in a fluidised bed, *Proc. Combust. Inst.*, 1982; 19; 1205 – 1212.
- [23] Hayhurst A N, Tucker R F, The combustion of carbon monoxide in a two-zone fluidized bed, *Combust. Flame* 1990; 79; 175 – 189.
- [24] Hayhurst A N, Does carbon monoxide burn inside a fluidized bed? *Combust. Flame* 1991; 85; 155 – 168.
- [25] Bulewicz E M, Żukowski W, Kandefer S, Pilawska M, Flame flashes when bubbles explode during the combustion of gaseous mixtures in a bubbling fluidized bed, *Combust. Flame* 2003; 132; 319 – 327.
- [26] Hayhurst A N, John J J, Wazacz R J, The combustion of propane and air as catalysed by platinum in a fluidised bed of hot sand, *Proc. Combust. Inst.*, 1998, 27, 3111 – 3118.

- [27] Żukowski W, A simple model for explosive combustion of premixed natural gas with air in a bubbling fluidized bed of inert sand, *Combust. Flame* 2003; 134; 399 – 409.
- [28] Darton R C, La Nauze R D, Davidson J F, Harrison D, Bubble growth due to coalescence in fluidized beds, *Trans I. Chem Engrs*, 1977; 55; 274 – 280.
- [29] Davidson J F, Harrison D, *Fluidised Particles*, Cambridge University Press, 1963, p. 95.
- [30] Warnatz J, Maas U, Dibble R W, *Combustion*, Springer, 1996, p. 138.
- [31] Griffiths J F, Barnard J A, *Flame and Combustion*, 3rd ed., Blackie, 1995, p. 159.
- [32] Chadeesingh D R, Hayhurst A N, The combustion of mixtures of methane and air in bubbling fluidized beds of hot sand, 19th FBC Conference, Vienna, 2006, 288 – 297.
- [33] Gaydon A G, Wolfhard H G, *Flames, their structure, radiation and temperature*, 4th Ed., Chapman & Hall, London, 1979, Ch. 8.
- [34] Baron J, Bulewicz E M, Kandefer S, Pilawska M, Żukowski W, Hayhurst A N, The combustion of polymer pellets in a bubbling fluidised bed *Fuel* 2006; 85; 2494 – 2508.
- [35] Rees A C, Davidson J F, Dennis J S, Hayhurst A N, The rise of a buoyant sphere in a gas-fluidized bed *Chem. Eng. Sci.* 2005; 60; 1143 – 1153.
- [36] Hayhurst A N, Neddderman R M, The burning of a liquid oil droplet, *Chemical Engineering Education* 1987; 21; 126 – 152.
- [37] Levenspiel O, *Engineering flow and heat exchange*, New York, Plenum; 1984, p. 200.
- [38] Parmar M S, Hayhurst A N, The heat transfer coefficient for a freely moving sphere in a bubbling fluidised bed *Chem. Eng. Sci.* 2002; 57; 3485 – 3494.
- [39] Kay and Laby, *Tables of Physical and Chemical constants*, Longman, Harlow, England, 15th Ed., p.69.

[40] Scott S A, Davidson J F, Dennis J S, Hayhurst A N, Heat transfer to a single sphere immersed in beds of particles supplied by gas at rates above and below minimum fluidization Ind. Eng. Chem. Res. 2004; 43; 5632 – 5644.

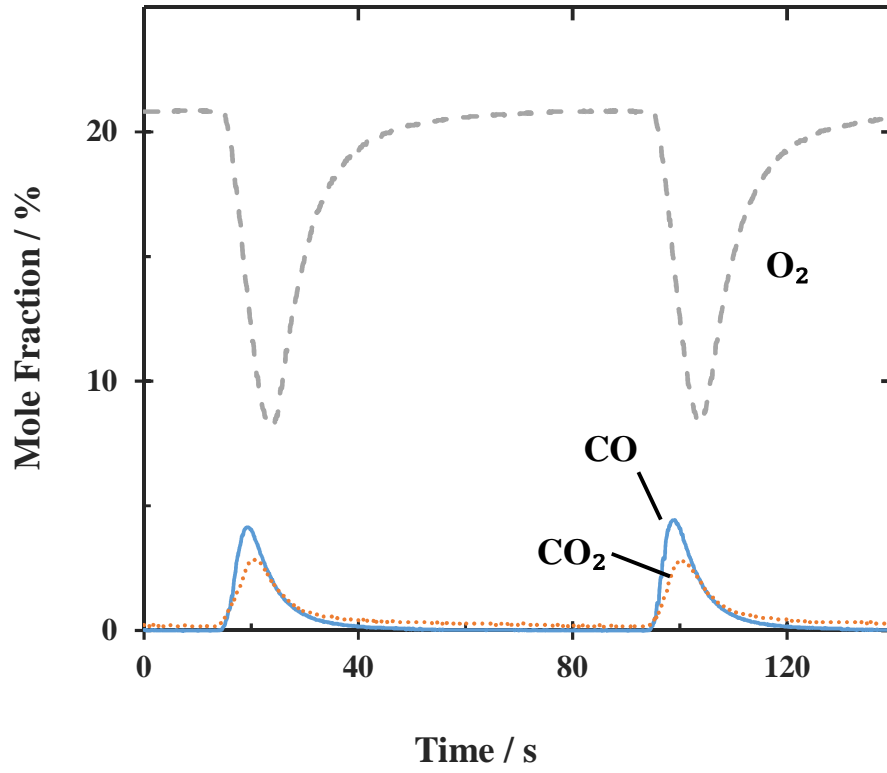


Fig. 1. Plots of the mole fractions of O_2 , CO and CO_2 in the off-gases versus time, as measured after two consecutive additions of 0.20 g of paraffin wax onto the top of a bed of alumina, when fluidised at 900°C by air with $U/U_{mf} = 2.6$.

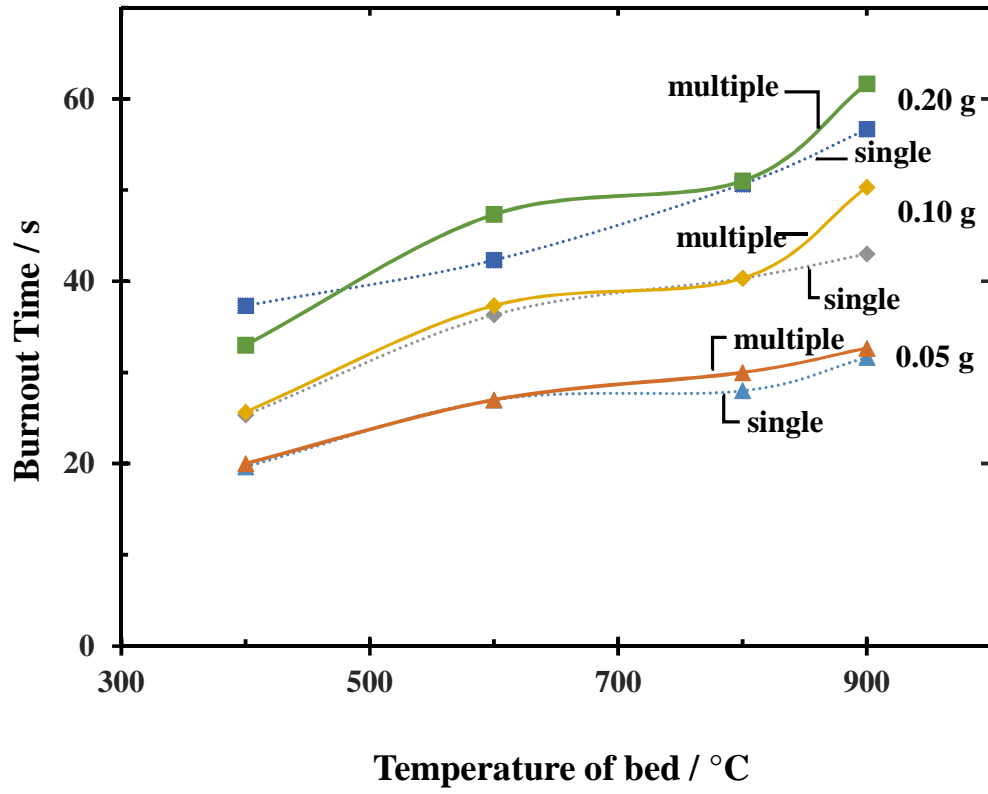


Fig. 2. Burn-out times measured in beds of different temperatures, but all with $U/U_{mf} = 2.6$. Also the mass of wax was 0.20, 0.10 or 0.05 g, added as either a single sphere or several smaller particles, dropped on top of the bed.

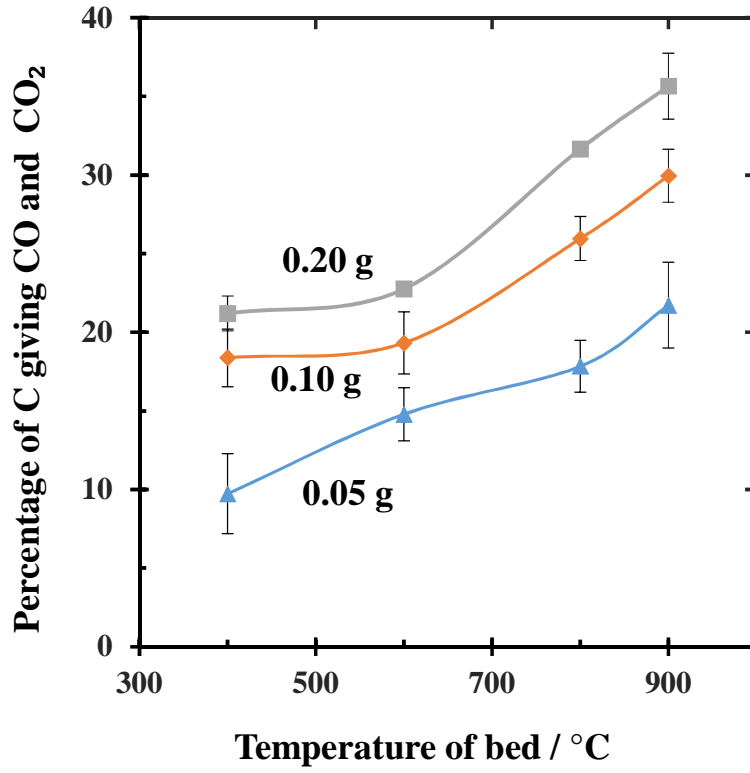


Fig. 3. The measured fraction of the carbon in a sample of paraffin wax, subsequently detected as CO or CO₂ in the off-gases. The mass of added wax was varied, as shown, as also was the temperature, but with $U/U_{mf} = 2.6$. The error bars represent one standard deviation.

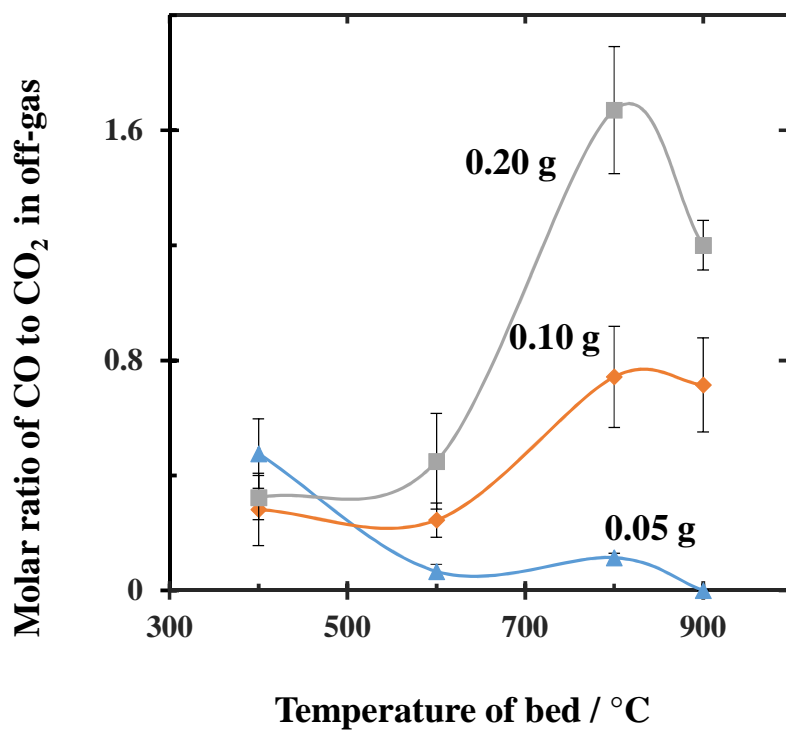


Fig. 4. Plots of the ratio of the total molar yields of CO and CO₂, in beds of different temperatures, for various amounts of wax added on top of the bed. Error bars denote one standard deviation.

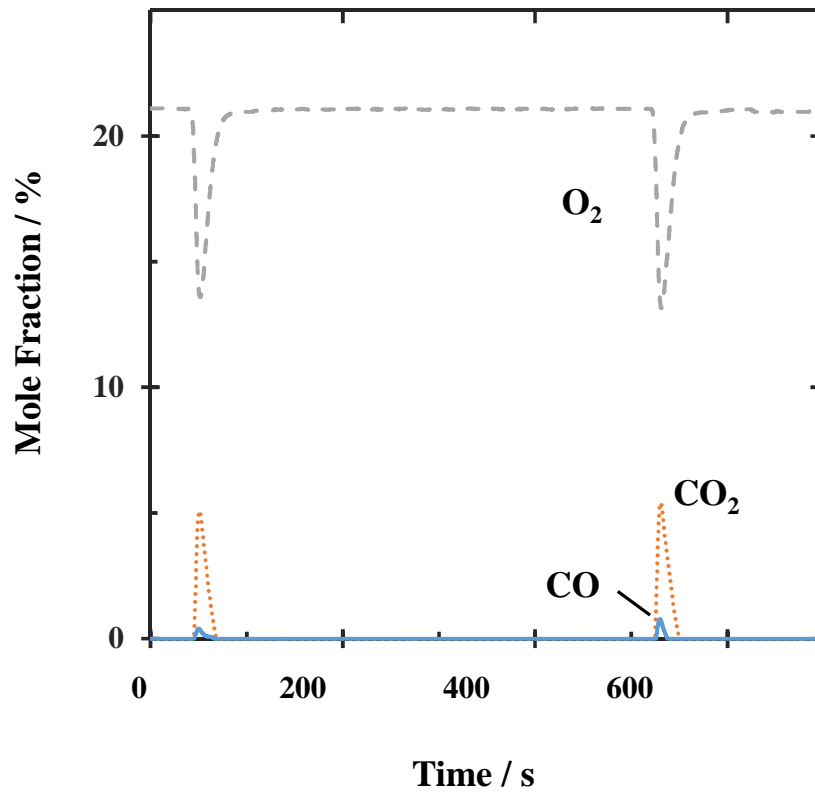


Fig. 5. Plots of the measured mole fractions of O_2 , CO and CO_2 against time, when two consecutive batches of 0.10 g of paraffin wax were added from the capsule to the middle of the bed at 800°C with $U/U_{mf} = 2.4$

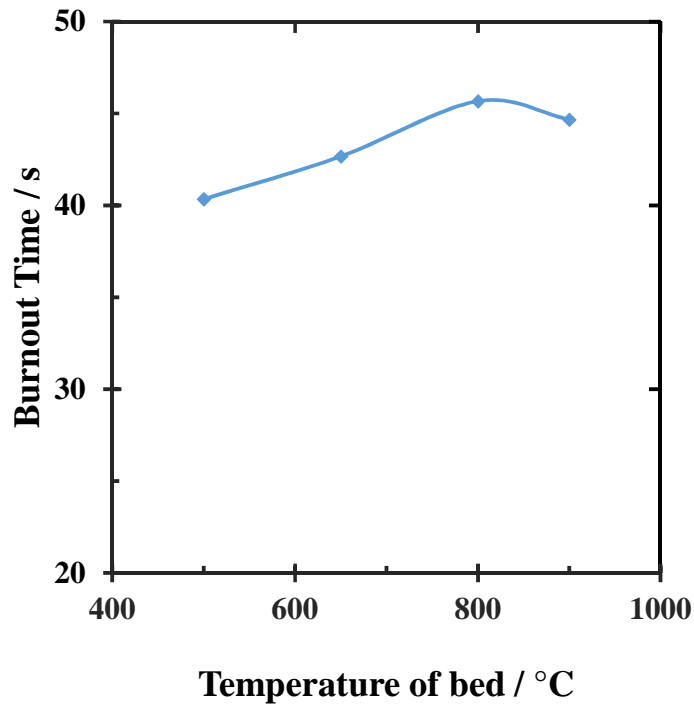


Fig. 6. Burn-out times measured for 0.10 g of paraffin wax added from the capsule to the middle of the bed in the range 500 to 900°C with $U/U_{mf} = 2.4$.

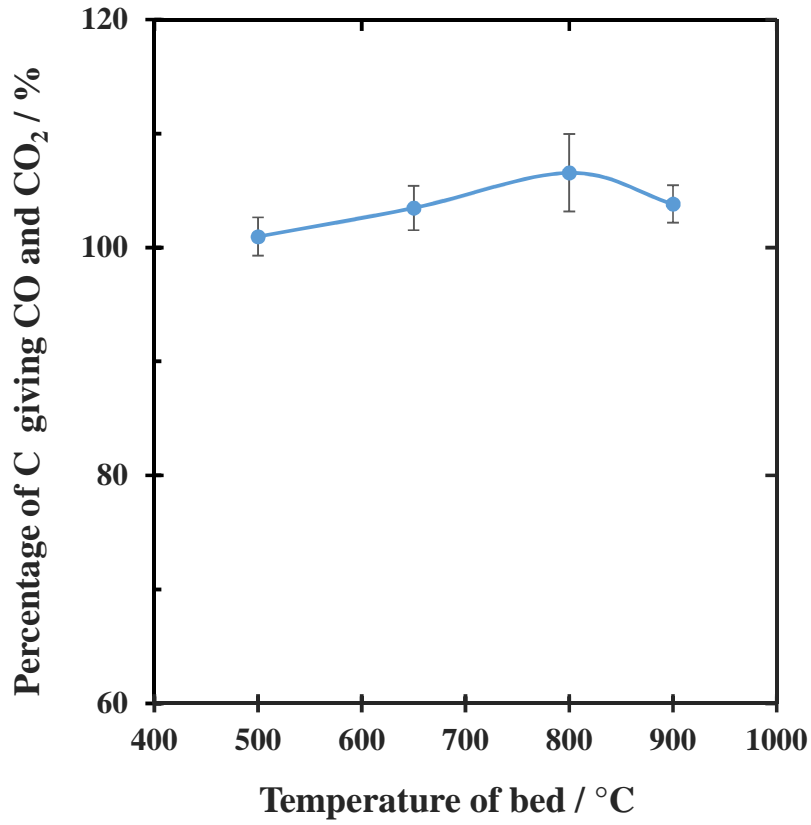


Fig. 7. Conversions of the carbon in paraffin wax to both CO and CO₂, when 0.10 g of the wax was added from the capsule to the middle of the bed at different temperatures with $U/U_{mf} = 2.4$.

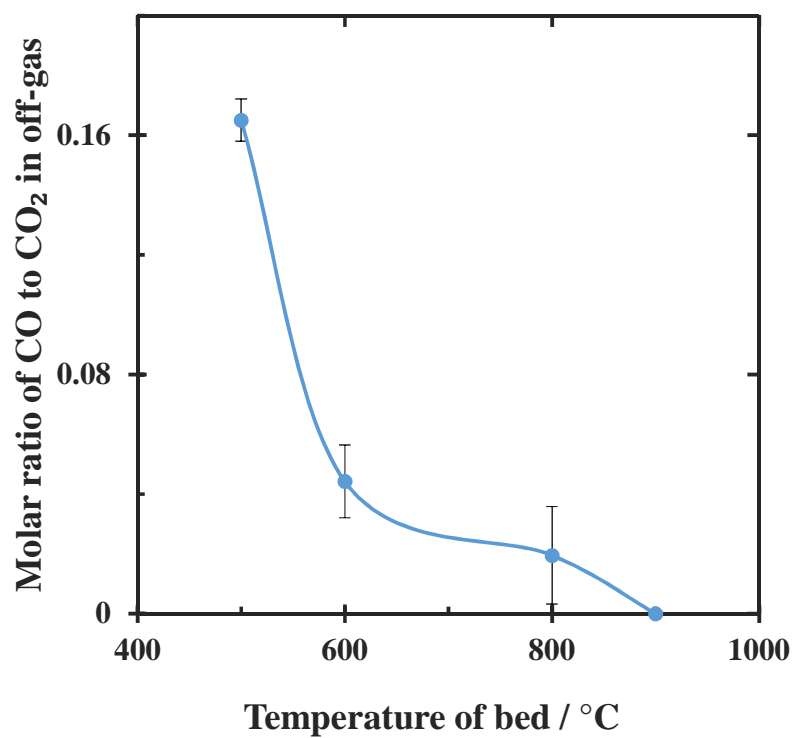


Fig. 8. Ratio of the total molar yields of CO and CO₂ in the off-gases after 0.10 g of paraffin wax had been added to the middle of the bed at different temperatures..

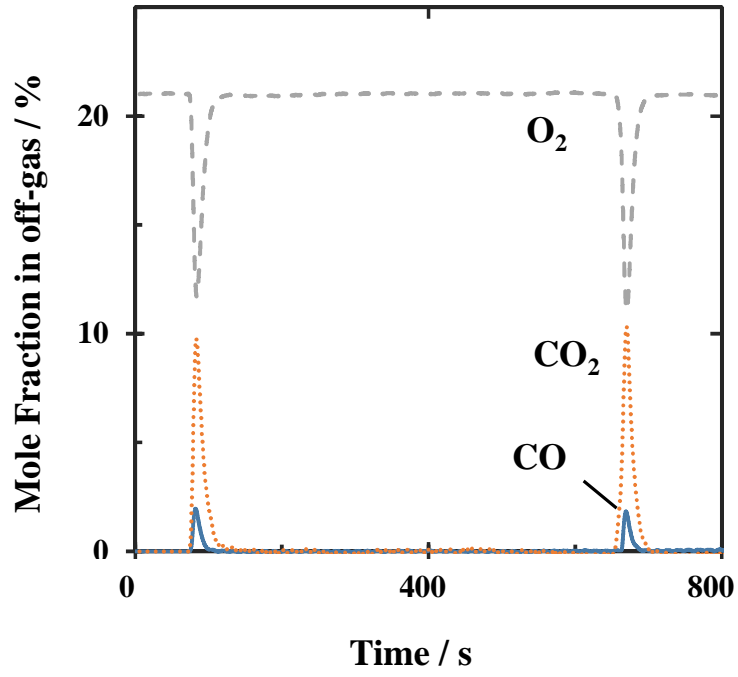


Fig. 9. Plots of the mole fractions of O_2 , CO and CO_2 after two consecutive additions of 0.30 g of glycerol from the steel capsule to the middle of the bed at 800°C with $U/U_{mf} = 2.4$.

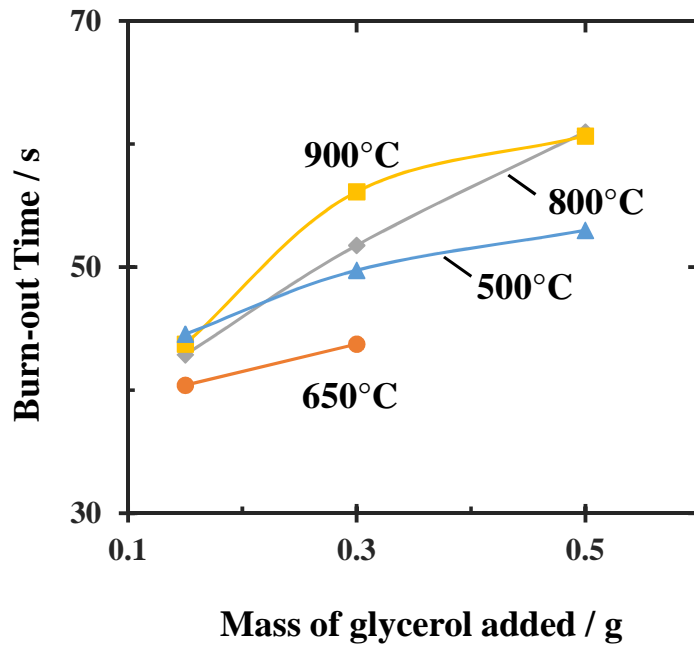


Fig. 10. Burn-out times for different masses of glycerol added to beds of different temperatures, all with $U/U_{mf} = 2.4$.

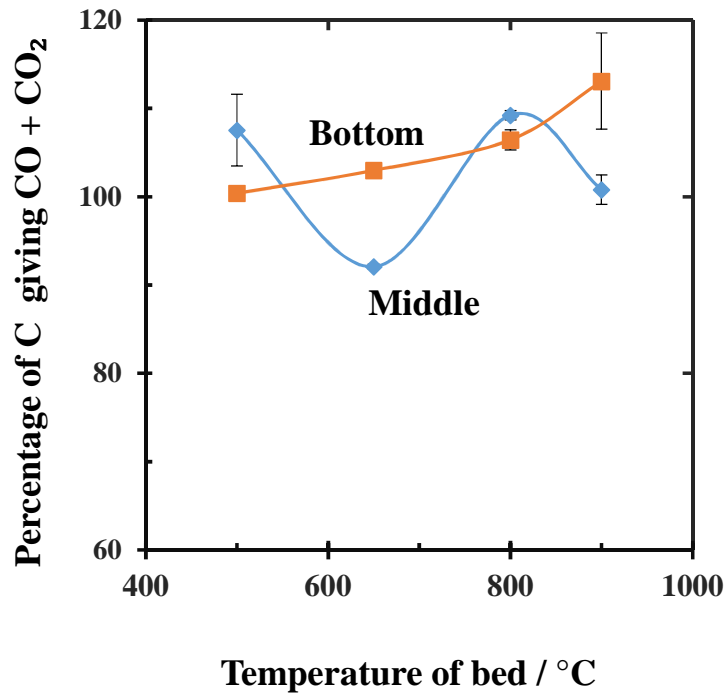


Fig. 11. The fraction of the carbon in the glycerol burned to CO or CO₂ after 0.30 g were added to the middle or bottom of the fluidised bed with $U/U_{mf} = 2.4$ at different temperatures.

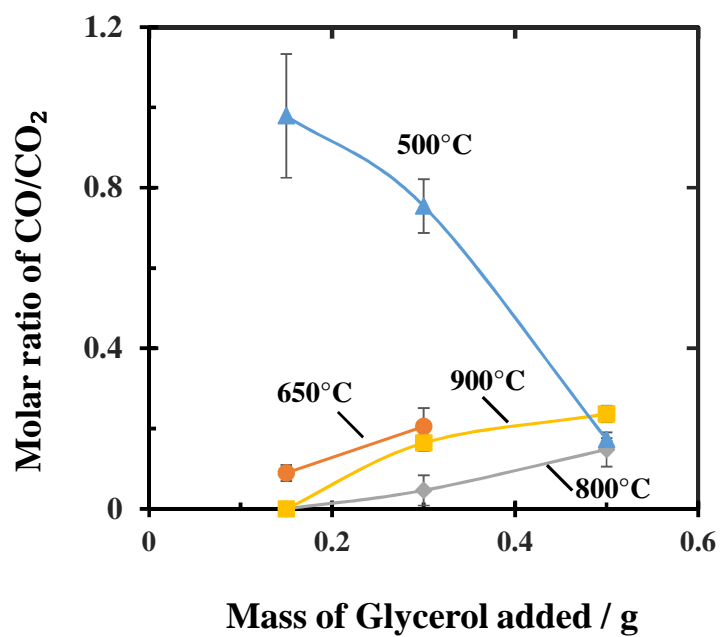


Fig. 12. Plots of the molar ratio of the total yields of CO and CO₂ after adding different masses of glycerol from the capsule to the middle of the fluidised bed at $U/U_{mf} = 2.4$.

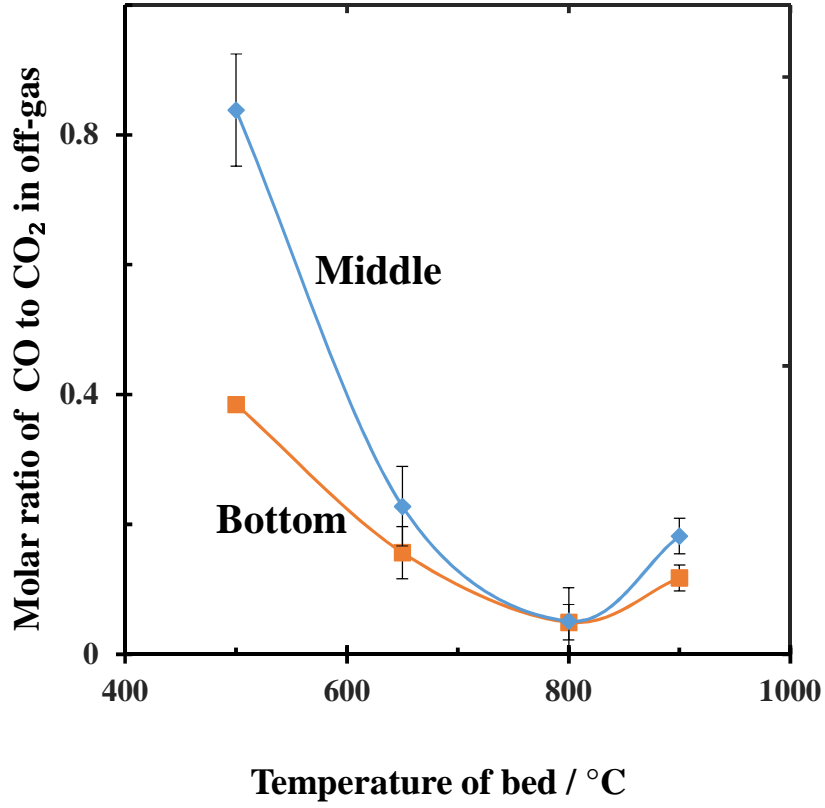


Fig. 13. Ratio of total molar yields of CO and CO₂ in the off-gas, after 0.30 g of glycerol was added to the bed at different temperatures, with $U/U_{mf} = 2.4$. The glycerol was added from the steel capsule, either at the bottom or middle of the bed. The error bars represent one standard deviation.

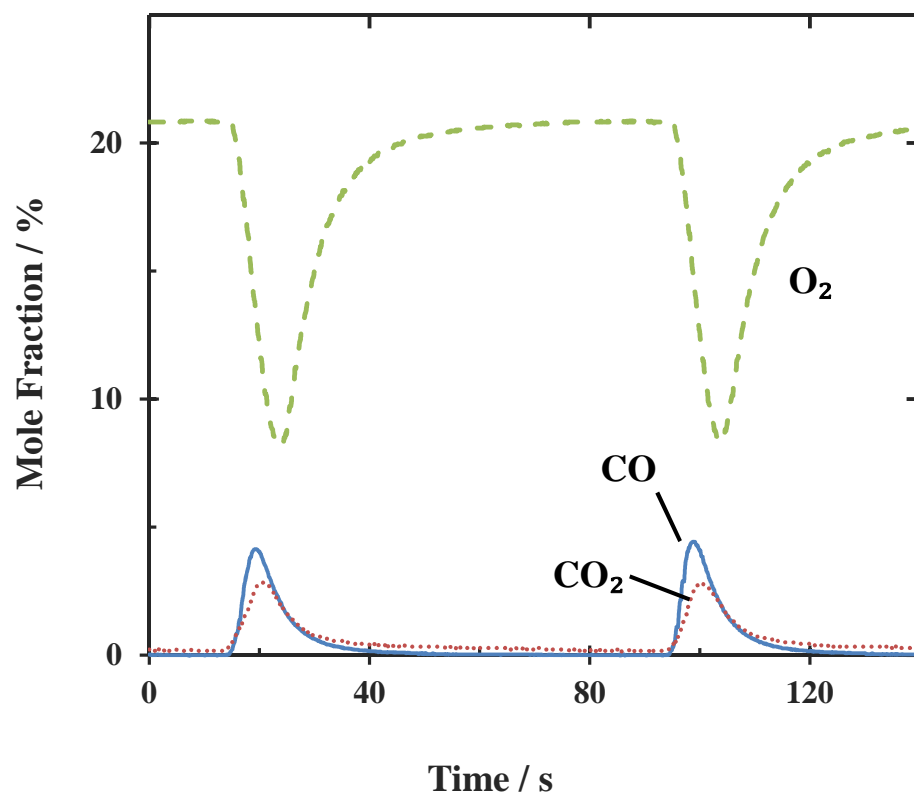


Fig. 1. Plots of the mole fractions of O_2 , CO and CO_2 in the off-gases versus time, as measured after two consecutive additions of 0.20 g of paraffin wax onto the top of a bed of alumina, when fluidized at 900°C by air with $U/U_{mf} = 2.6$.

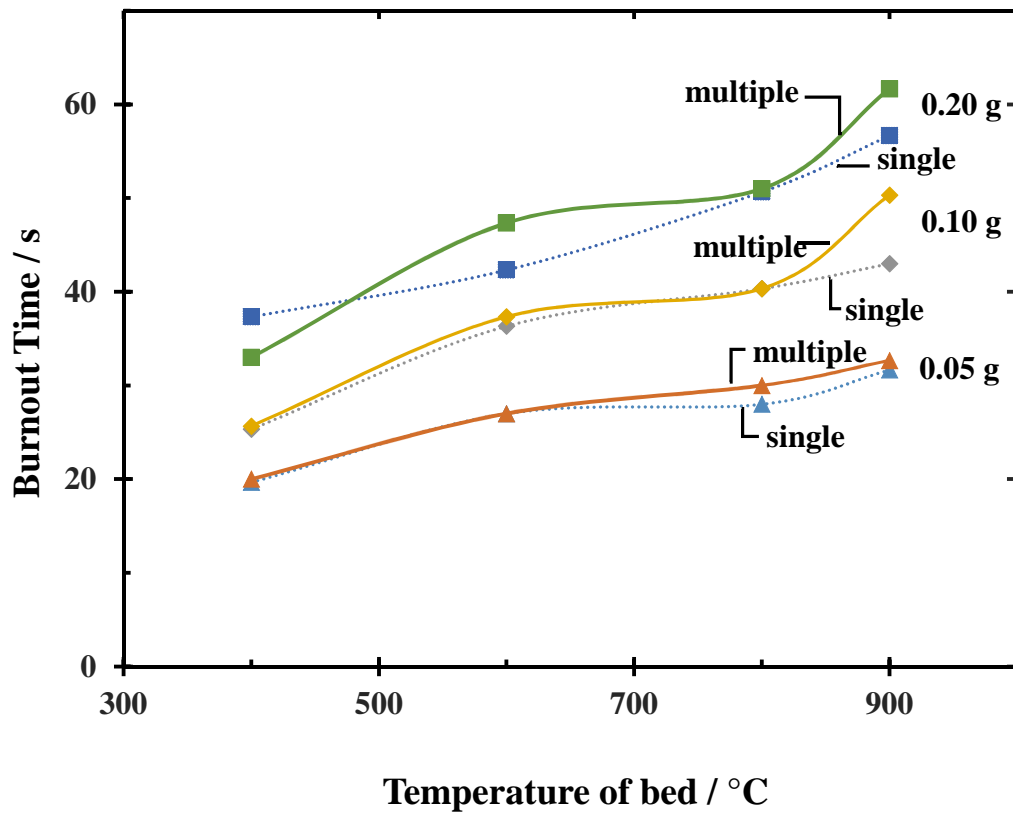


Fig. 2. Burn-out times measured in beds of different temperatures, but all with $U/U_{mf} = 2.6$. Also the mass of wax was 0.20, 0.10 or 0.05 g, added as either a single sphere or several smaller particles, dropped on top of the bed.

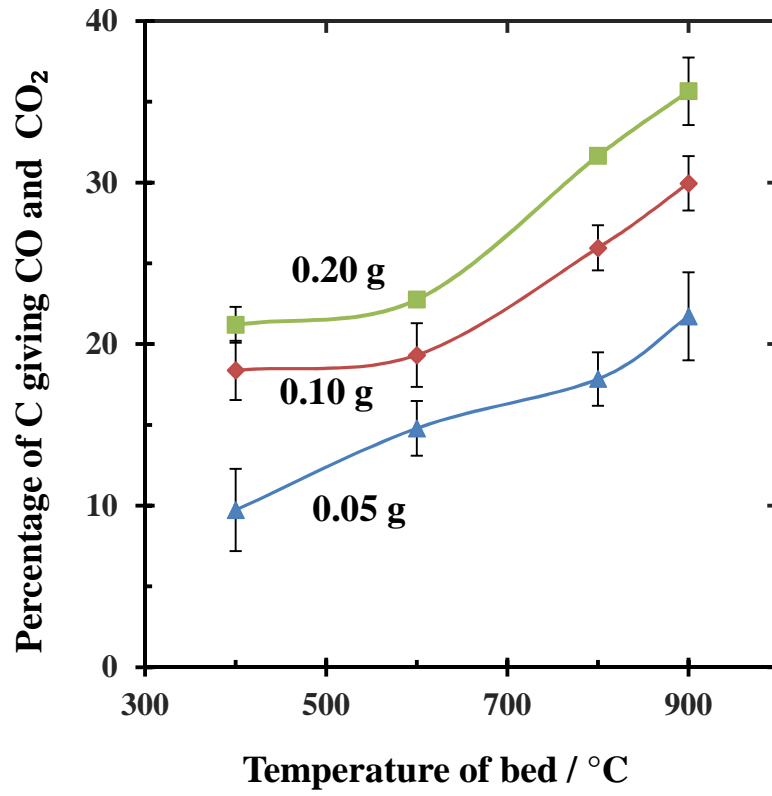


Fig. 3. The measured fraction of the carbon in a sample of paraffin wax, subsequently detected as CO or CO₂ in the off-gases. The mass of added wax was varied, as shown, as also was the temperature, but with $U/U_{mf} = 2.6$. The error bars represent one standard deviation.

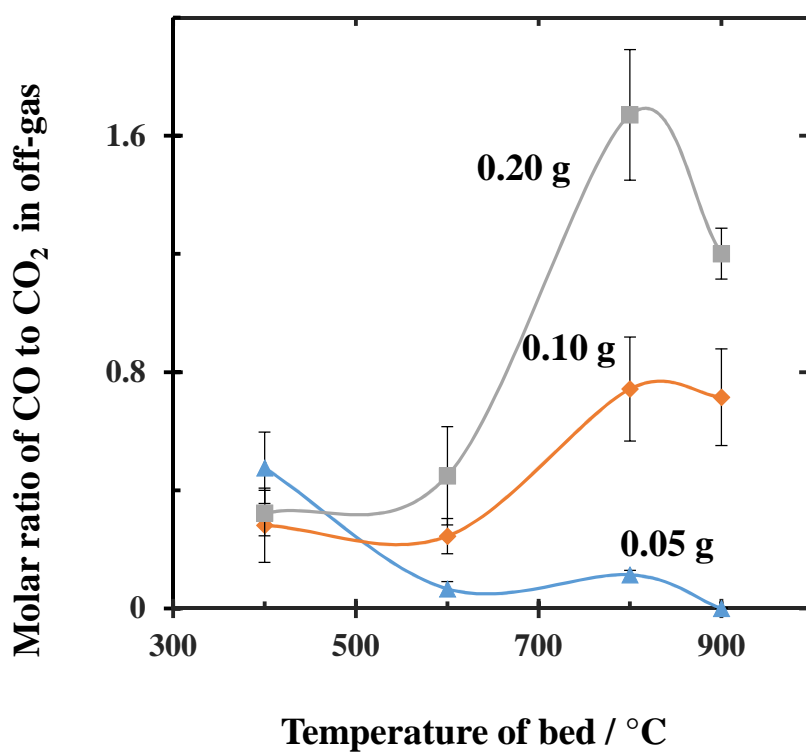


Fig. 4. Plots of the ratio of the total molar yields of CO and CO₂, in beds of different temperatures, for various amounts of wax added on top of the bed. Error bars denote one standard deviation.

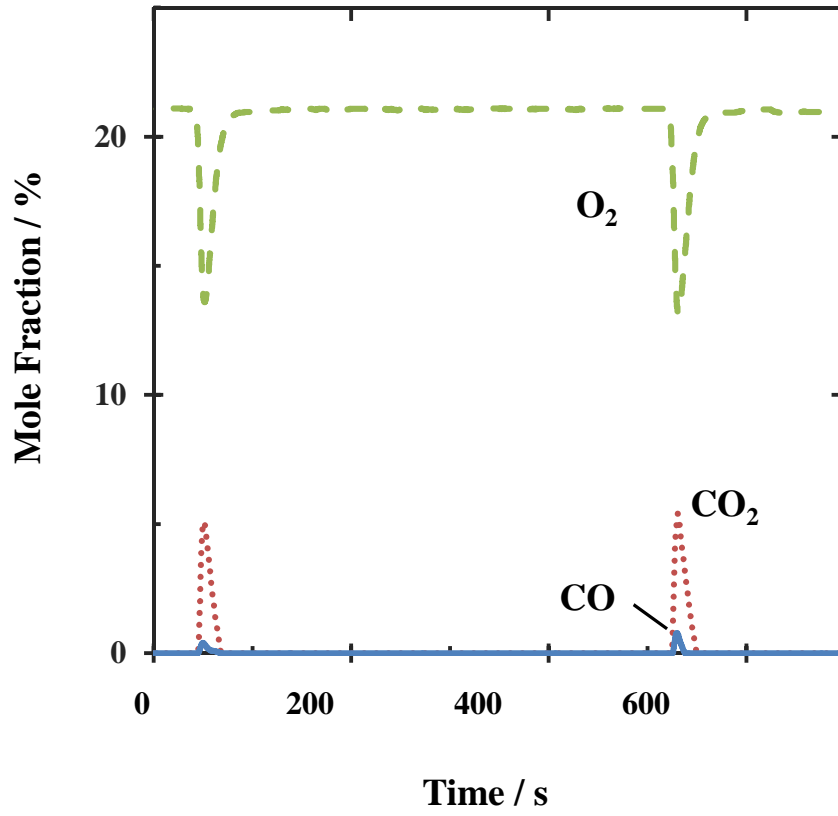


Fig. 5. Plots of the measured mole fractions of O_2 , CO and CO_2 against time, when two consecutive batches of 0.10 g of paraffin wax were added from the capsule to the middle of the bed at 800°C with $U/U_{mf} = 2.4$

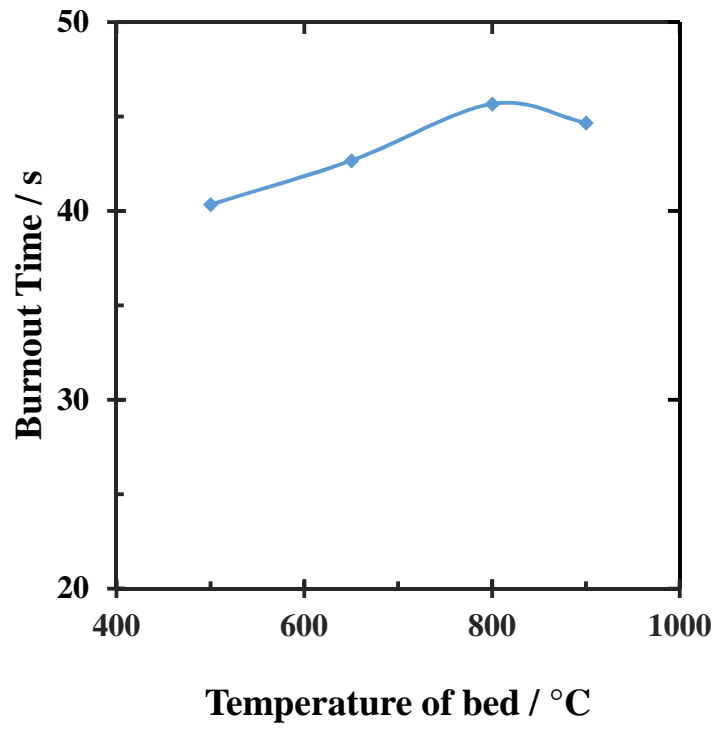


Fig. 6. Burn-out times measured for 0.10 g of paraffin wax added from the capsule to the middle of the bed in the range 500 to 900°C with $U/U_{mf} = 2.4$.

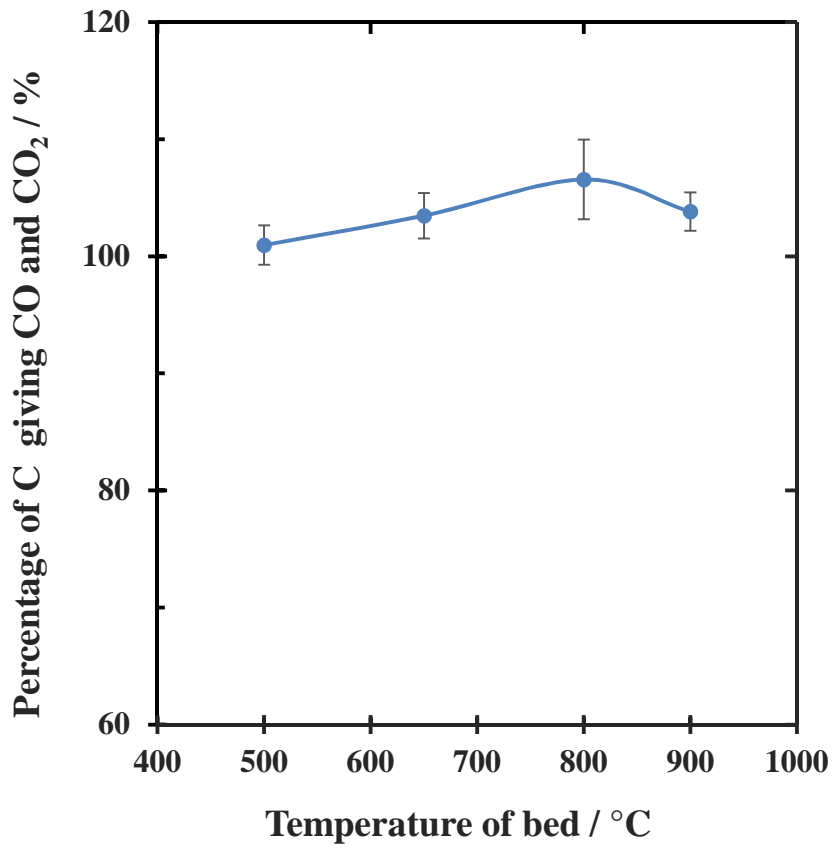


Fig. 7. Conversions of the carbon in paraffin wax to both CO and CO₂, when 0.10 g of the wax was added from the capsule to the middle of the bed at different temperatures with $U/U_{mf} = 2.4$.

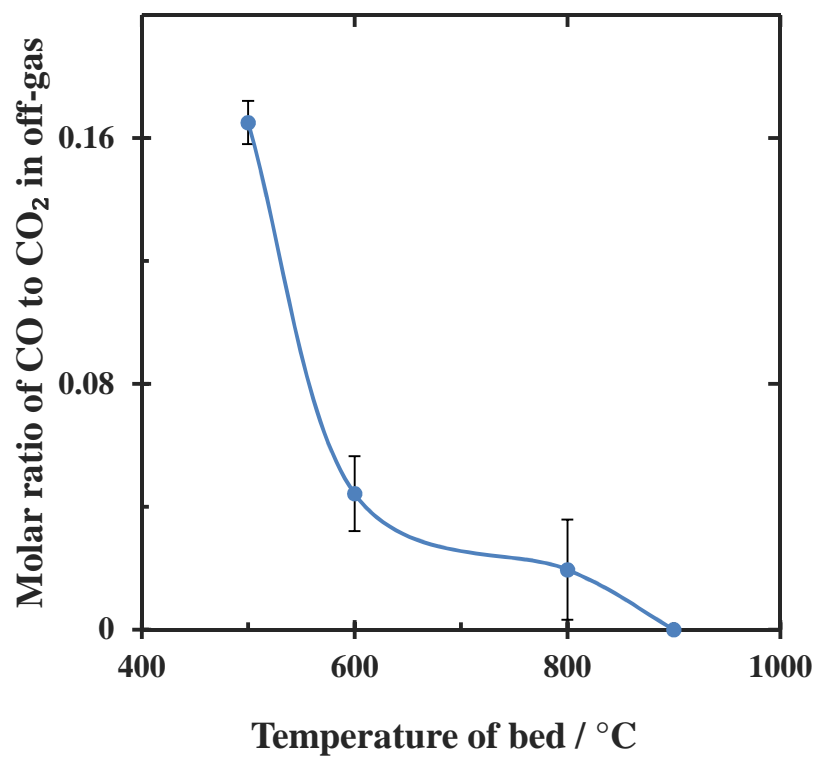


Fig. 8. Ratio of the total molar yields of CO and CO₂ in the off-gases after 0.10 g of paraffin wax had been added to the middle of the bed.

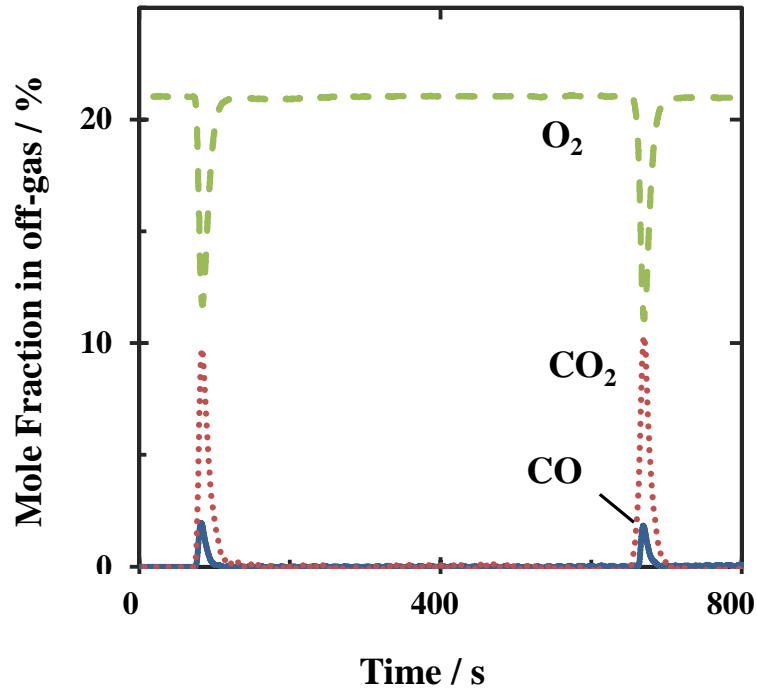


Fig. 9. Plots of the mole fractions of O_2 , CO and CO_2 after two consecutive additions of 0.30 g of glycerol from the steel capsule to the middle of the bed at 800°C with $U/U_{mf} = 2.4$.

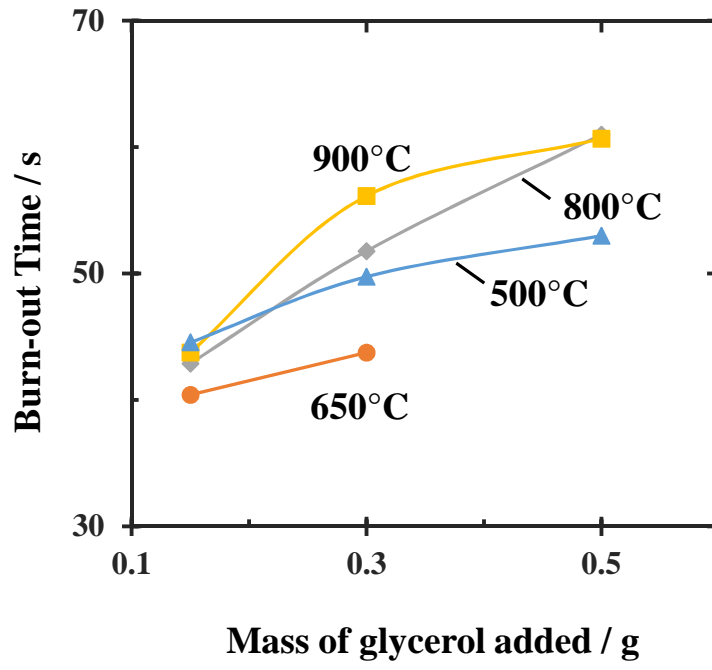


Fig. 10. Burn-out times for different masses of glycerol added to beds of different temperatures, all with $U/U_{mf} = 2.4$.

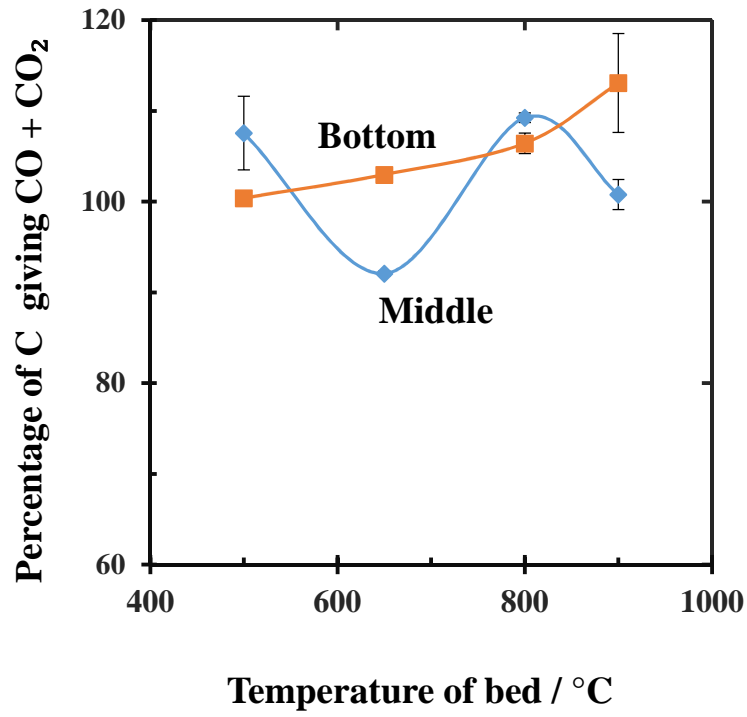


Fig. 11. The fraction of the carbon in the glycerol burned to CO or CO₂ after 0.30 g were added to the middle or bottom of the fluidised bed with $U/U_{mf} = 2.4$.

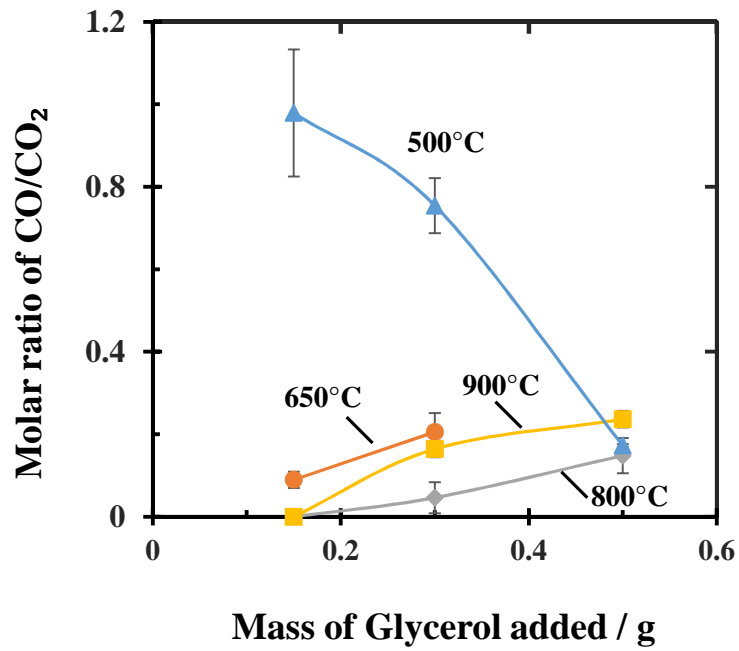


Fig. 12. Plots of the molar ratio of the total yields of CO and CO₂ after adding different masses of glycerol from the capsule to the middle of the fluidised bed at $U/U_{mf} = 2.4$.

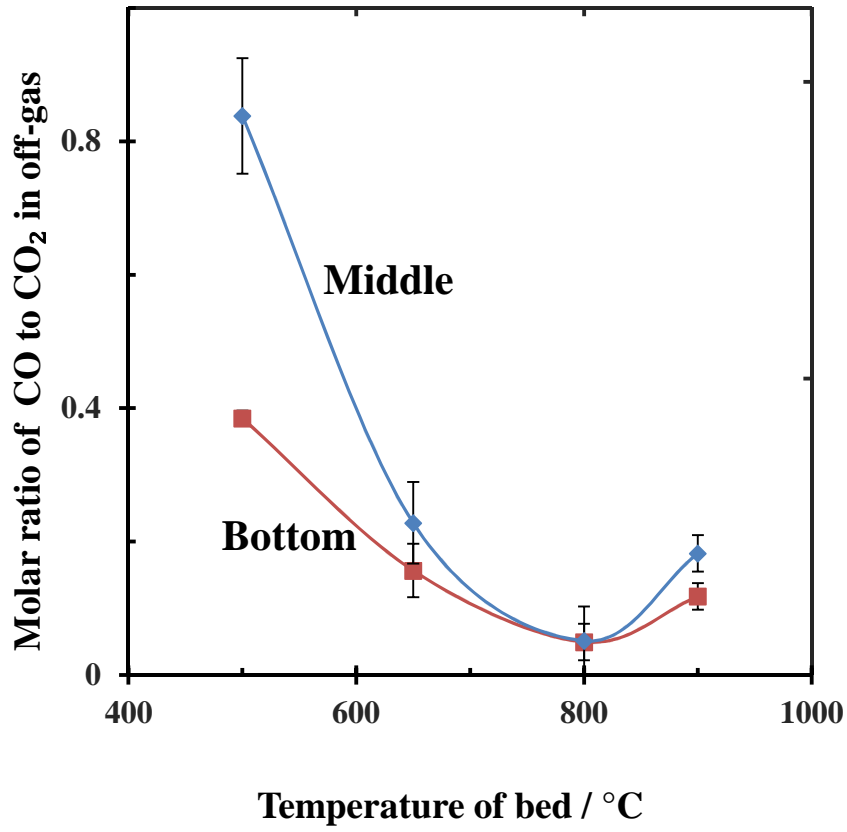


Fig. 13. Ratio of total molar yields of CO and CO₂ in the off-gas, after 0.30 g of glycerol was added to the bed at different temperatures, with $U/U_{mf} = 2.4$. The glycerol was added from the steel capsule, either at the bottom or middle of the bed. The error bars represent one standard deviation.